Available online at www.sciencedirect.com
ScienceDirect
Journal of Solid State Chemistry 181 (2008) 1377–1386
JOURNAL OF SOLID STATE CHEMISTRY
www.elsevier.com/locate/jssc

Cation disorder and phase transitions in the four-layer ferroelectric Aurivillius phases $ABi_4Ti_4O_{15}$ (A = Ca, Sr, Ba, Pb)

Brendan J. Kennedy[a,*], Qingdi Zhou[a], Ismunandar[b], Yoshika Kubota[c], Kenichi Kato[d]

[a]*School of Chemistry, The University of Sydney, Sydney, NSW 2006, Australia*
[b]*Inorganic and Physical Chemistry Division, Faculty of Mathematics and Natural Sciences, Institut Teknologi Bandung, Jl. Ganesa 10, Bandung 40132, Indonesia*
[c]*Department of Physical Science, Graduate School of Science, Osaka Prefecture University, Sakai, Osaka 599-8531, Japan*
[d]*RIKEN SPring-8 Center, 1-1-1 Kouto, Sayo-cho, Sayo-gun, Hyogo 679-5148, Japan*

Received 30 October 2007; received in revised form 29 January 2008; accepted 13 February 2008
Available online 4 March 2008

Abstract

Crystal structures of a series of bi-layered compounds $ABi_4Ti_4O_{15}$ (A = Ca, Sr, Ba, Pb) have been investigated using a combination of synchrotron X-ray and neutron powder diffraction data. All four oxides adopt an orthorhombic structure at room temperature and the structures have been refined in space group $A2_1am$. This orthorhombic structure is a consequence of a combination of rotation of the TiO_6, resulting from the less than optimal size of the A-type cation, and displacement of the Ti atoms towards the Bi_2O_2 layers. There is partial disorder of the Bi and A-type cations over two of the three available sites, which increases in the order Ca < Sr and Pb < Ba.

Keywords: Phase transition; Aurivillius phase

1. Introduction

Layered bismuth oxides have attracted considerable interest over the past decade due to the rich variety of technologically important properties displayed by such oxides [1–5]. Some of the most intense studies have been directed towards the Aurivillius type oxides [6] that have the general formula $[Bi_2O_2][A_{n-1}B_nO_{3n+1}]$ $n = 1, 2, 3, 4$ where the $[Bi_2O_2]^{2+}$ layers are interwoven with perovskite-like $[A_{n-1}B_nO_{3n+1}]^{2-}$ layers. The $n = 2$ oxides, $[Bi_2O_2][AB_2O_7]$, or more commonly written as $ABi_2B_2O_9$, with A = Ca, Sr, Ba, Pb and B = Nb, Ta have attracted the most attention since systems based on $SrBi_2Ta_2O_9$ have been identified as amongst the most promising materials for use in non-volatile memory applications (ferroelectric random access memories: FeRAMs) [7].

Four observations can be made from the recent comprehensive studies [8–14] reported for the $n = 2$ Aurivillius oxides $ABi_2B_2O_9$, namely:

1. There is considerable disorder between the perovskite A-type and layer Bi atoms.
2. Reduction in the size of the A-type cation induces tilting of the BO_6 octahedra analogous to that seen in perovskites.
3. The observed ferroelectric properties are a consequence of displacement of the perovskite A- and B-type cations relative to the Bi_2O_2 layers.
4. The transition from the low temperature ferroelectric phase to the high temperature paraelectric phase apparently only involves continuous phase transition(s).

By comparison with the $n = 2$ oxides relatively little is known about the $n = 4$ Aurivillius oxides $ABi_4Ti_4O_{15}$ [15–17]. Aurivillius originally described $BaBi_4Ti_4O_{15}$ as being tetragonal at room temperature, whereas the remaining oxides (A = Ca, Sr, Pb) are described as orthorhombic [6]. Irie and co-workers suggested [18] that $BaBi_4Ti_4O_{15}$ is in fact orthorhombic although they did not present any detailed structural information. Kojima

*Corresponding author. Fax: +61 2 9351 3329.
E-mail address: B.Kennedy@chem.usyd.edu.au (B.J. Kennedy).

0022-4596/$ - see front matter © 2008 Elsevier Inc. All rights reserved.
doi:10.1016/j.jssc.2008.02.015

[19] noted that the Raman modes in $BaBi_4Ti_4O_{15}$ are broader than in the analogous Ca, Sr or Pb compounds and suggested that this may be due to cation disorder, where some of the Ba ions randomly occupy the Bi sites of the perovskite-like layers. By analogy with the $n = 2$ oxides the Ba compound is expected to have the greatest degree of cation disorder [11,13]. Using single crystal X-ray diffraction methods Tellier et al. [20] showed that $CaBi_4Ti_4O_{15}$ is orthorhombic in $A2_1am$ with the A-type cations displaced along the polar a-axis. These authors also confirmed our earlier work [21] that showed $BaBi_4Ti_4O_{15}$ is also orthorhombic in the same space group, although in their refinements they restrained the cations to their equivalent $Fmmm$ positions. Recently Hervoches et al. [22] also described the structure of $SrBi_4Ti_4O_{15}$ using both X-ray and neutron diffraction methods. In this work they confirmed the orthorhombic structure of $SrBi_4Ti_4O_{15}$ and suggested the material undergoes two phase transitions $A2_1am \rightarrow Amam \rightarrow I4/mmm$ as the temperature is increased, apparently confirming the earlier conclusions of Kojima et al. [19] and Reaney and Damjanovic [23] on the existence of such high temperature phase transitions. Nalini and Guru Row [17] also reported evidence that $SrBi_4Ti_4O_{15}$ transforms to the tetragonal structure upon heating, but concluded that $PbBi_4Ti_4O_{15}$ does not display any structural phase transitions below 873 K. The sequence of phase transitions postulated by Hervoches et al. [22] for $SrBi_4Ti_4O_{15}$ is the same as that observed in the $n = 2$ oxides $SrBi_2Ta_2O_9$ [9] and $PbBi_2B_2O_9$ $B =$ Nb, Ta [10]. Macquart et al. [9] have shown these two transitions are allowed to be continuous. However, the work of Hervoches [22] on $SrBi_4Ti_4O_{15}$ relied on very coarse temperature intervals and no conclusions about the nature of the phase transition are possible from this published work. Surprisingly Hervoches et al. [22] concluded that there was no significant occupancy of the $[Bi_2O_2]$ layers by Sr and that the Sr was randomly distributed over the two perovskite-like A-sites. Tellier et al. [20] concluded that although Ba is partially disordered into the Bi_2O_2 layers, the Ca in $CaBi_4Ti_4O_{15}$ is not. In the $n = 2$ oxides disorder of the A-cation into the $[Bi_2O_2]$ layers plays an important role in optimizing atomic spacing between this and the perovskite-like layers [13,14].

In a continuation of our studies of phase transitions in Aurivillius type oxides, including the $n = 5$ oxides $[A_2Bi_4Ti_5O_{18}]$ [24] the present paper describes the structure of the four oxides $ABi_4Ti_4O_{15}$ $A =$ Ca, Sr, Ba, Pb obtained from analysis of a combination of powder synchrotron X-ray and neutron diffraction data. The temperature dependencies of the structures are also presented.

2. Experimental

Polycrystalline samples of the four oxides $ABi_4Ti_4O_{15}$ ($A =$ Ca, Sr, Ba, Pb) were prepared by the solid state reaction of an intimate mixture of ACO_3, Bi_2O_3 and TiO_2 in the correct stoichiometric proportions. The samples were heated at 750, 950 and 1050 °C for 24 h each with intermittent grinding after each heating step. All samples were slow cooled in air. Powder X-ray diffraction data, collected using a Siemens D5000 diffractometer employing Cu $K\alpha$, radiation showed the cream-colored samples to be single phase and highly crystalline. The synchrotron X-ray diffraction patterns were measured using a monochromatic wavelength of 0.85039 Å with the large Debye–Scherrer diffractometer at beamline 20 B at the Photon Factory at KEK, Tsukuba Japan [25]. The samples were housed in 0.3 mm dia capillaries and rotated during the measurements to minimize preferred orientation effects. Variable temperature synchrotron diffraction patterns were recorded at Beamline BL02B2 at SPring-8 [26]. For these measurements the samples were sealed in 0.2 mm dia quartz capillaries, and the wavelength of the incident beam was 0.5010 Å. The temperature was controlled using a N_2 gas flow system to within 0.2° of the set point with an estimated accuracy of ±2°. The temperature at the sample position was calibrated using a standard thermocouple and this was checked against phase transitions in $PbTiO_3$ and $BaTiO_3$.

The neutron powder diffraction data were collected on the high-resolution powder diffractometer at the Australian Nuclear Science and Technology Organization research reactor at Lucas Heights [27]. The wavelength used was 1.4925 Å and the data were collected in 0.05° steps over the 2θ range 5–150°. The samples were held in vanadium containers and were rotated around their vertical axis during these measurements. The structures were refined using the RIETICA package [28].

2.1. Structure refinement

Examination of the room temperature synchrotron diffraction data confirmed single phase samples had been obtained for the four oxides, with the exception that weak peaks due to the presence of small amounts of a pyrochlore phase were observed in the two synchrotron diffraction patterns for $SrBi_4Ti_4O_{15}$ (SBT-4). We note that the X-ray diffraction pattern of $BaBi_4Ti_4O_{15}$ (BBT-4) recorded using a conventional diffractometer, can be well fitted in a tetragonal structure, and indeed a number of authors [17,18] have suggested that, as occurs in the analogous $n = 2$ oxide $BaBi_2Nb_2O_9$, [11,29] this has the non-polar space group $I4/mmm$. Examination of both the synchrotron X-ray and neutron diffraction patterns did not reveal any reflections forbidden in $I4/mmm$ such as the 015 or 215 reflections, however, as is illustrated in Fig. 1, the higher resolution synchrotron diffraction data shows the choice of this tetragonal space group is clearly incorrect, and that the structure is in fact orthorhombic. Furthermore the reported [16] ferroelectric properties of BBT-4 are incompatible with space group $I4/mmm$.

As noted above Tellier et al. [20] also concluded that BBT-4 has orthorhombic symmetry, and presented Selected Area Electron Diffraction data to support this. The reflections indicative of orthorhombic symmetry are associated with the tilting of the TiO_6 octahedra and the tilting of the octahedra are much smaller in the Ba

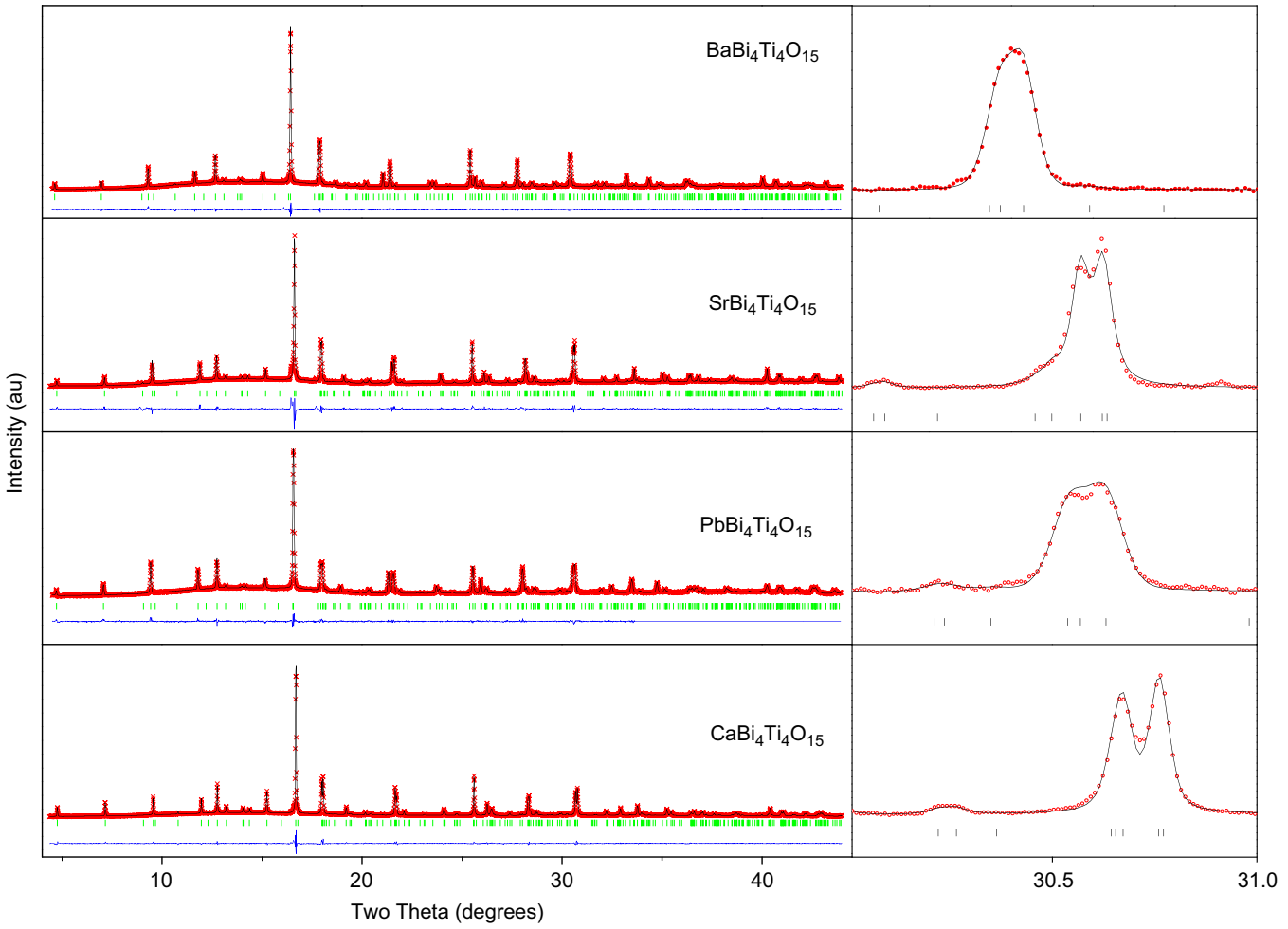

Fig. 1. Observed, calculated and difference synchrotron X-ray diffraction profiles for the four oxides $ABi_4Ti_4O_{15}$ A = Ca, Sr, Ba and Pb. The structures were refined in the orthorhombic space group $A2_1am$. The panels to the right illustrates the splitting of the tetragonal 110 reflection into the 200/020 orthorhombic doublet. The orthorhombic 0 1 13 reflection also appears in this region.

compound compared to the other three oxides studied. Indeed for A = Ca, Sr and Pb we observe a diagnostic 015 reflection near $d = 4.6$ Å in the synchrotron and the 215 reflection near $d = 2.34$ Å in the neutron diffraction patterns. Both these reflections are forbidden in $I4/mmm$. In passing it is worth noting that the R-factors for the Rietveld-refinement for the synchrotron data in the orthorhombic and tetragonal models for BBT-4 were reasonably similar (R_p 2.62, R_{wp} 3.60 in $I4/mmm$ vs R_p 2.19 and R_{wp} 2.82 in $A2_1am$ for the 0.85 Å synchrotron data) and demonstrate the inappropriateness of relying on R-factors alone to distinguish between structural models.

Having established that the structures of the four oxides are orthorhombic the structures were then refined in space group $A2_1am$ using the results reported for SBT-4 by Hervoches et al. [22] as a starting model for the refinements. Following Hervoches et al. [22] it was initially assumed that the Bi_2O_2 layers did not contain any A-type cation but rather that the A-type cation was randomly distributed over the two remaining sites. The initial refinements were undertaken using the two synchrotron X-ray diffraction data sets and assumed that the displacement parameters of the oxygen atoms were all equal. Removal of this restraint resulted in unstable refinements and/or physically unreasonable parameters. In all cases these refinements were generally satisfactory, with the exception of some anomalous displacement parameters associated with the cations. At that stage the possibility of cation disorder was considered for all oxides, except A = Pb. For both the 0.5 and 0.85 Å X-rays the scattering factors of Bi^{3+} and Pb^{2+} are sufficiently similar to make these elements indistinguishable. Attempts to obtain a precise description of the cation disorder in the samples proved fruitless, with no systematic variation in the site occupancies being apparent. It is well known that the displacement parameters and site occupancy factors are highly correlated in structural refinements, and examination of the correlation matrix produced during the Rietveld refinement confirmed this. What was unexpected was the strong correlation between the oxygen displacement parameters and the cation (Bi/A) occupancies. Correlations of up to 40% were observed. As a consequence of these correlations obtaining a precise description of the cation disorder solely using the X-ray diffraction data was not possible.

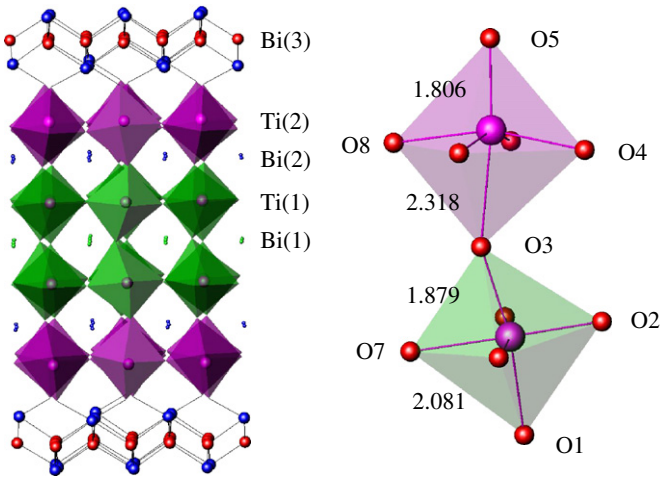

Fig. 2. Representation of the structure of the $n = 4$ Aurivillius oxides $ABi_4Ti_4O_{15}$ A = Ca, Sr, Ba and Pb. The diagram illustrates both the titling of the TiO_6 octahedra and the displacement of the ions along the a-axis. The distances given are those observed for CBT-4.

Ultimately the structures were refined using a combination of the two synchrotron and the neutron diffraction data sets. By including the neutron diffraction data it was possible to refine the oxygen positional parameters and independent displacement parameters for each of the crystallographically unique oxygen atoms. Equally importantly by including the neutron diffraction data in the refinement the correlations between the site occupancies and oxygen displacement parameters were well below 10% allowing the cation disorder to be probed. In these refinements it was assumed that the positions and displacement parameters for the cations (Bi and A) occupying the same sites were equal and that all the sites were fully occupied. In these refinements the refined occupancies of the Bi(3) site by Ca in CBT-4 and of the Bi(1) site by Pb in PBT-4 were observed to be less than unity and these were fixed at zero in the final refinements. See Fig. 2 for the locations of the Bi(1), Bi(2) and Bi(3) sites. The fitted synchrotron X-ray and neutron diffraction

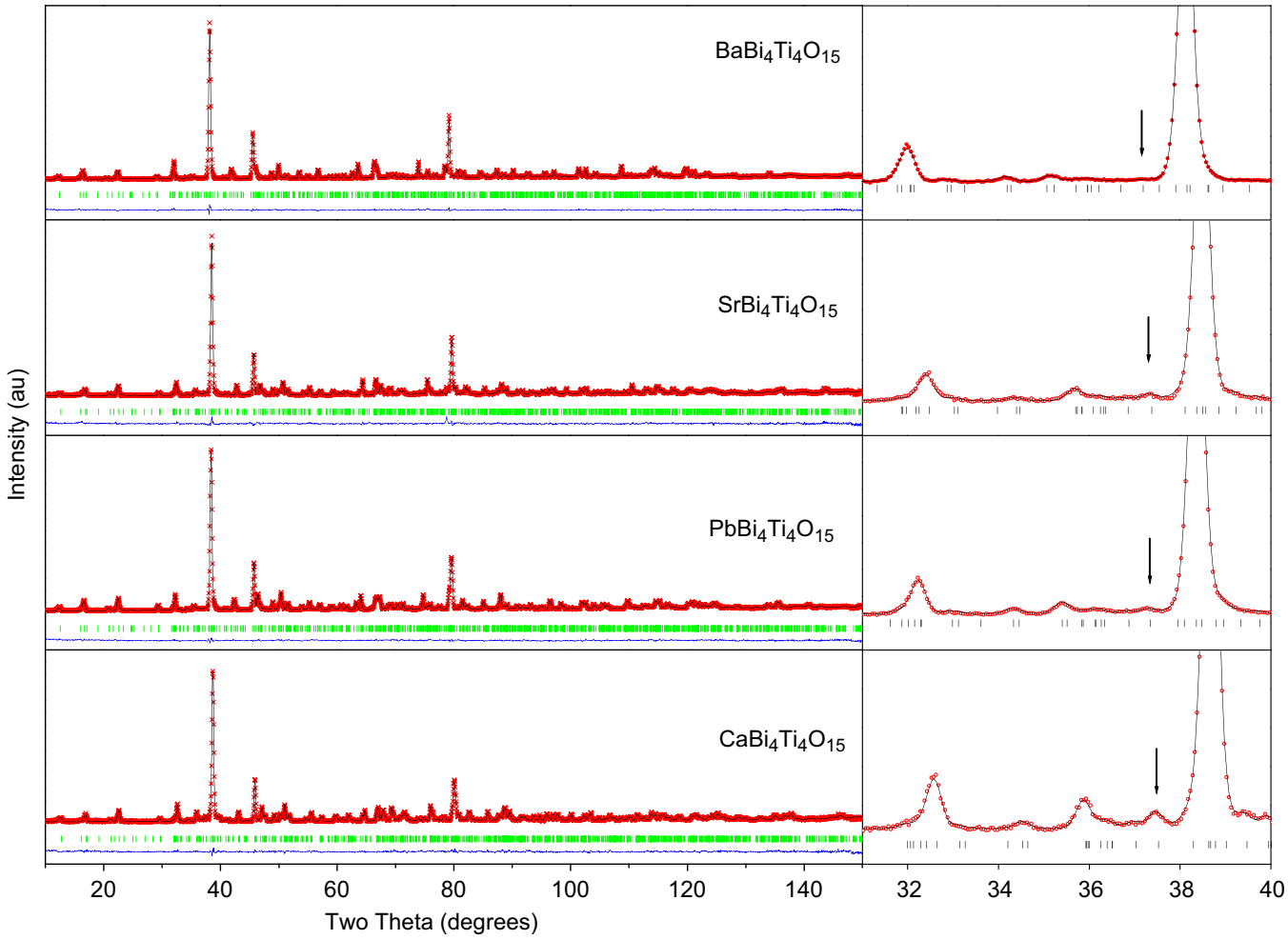

Fig. 3. Observed, calculated and difference neutron diffraction profiles for the four oxides $ABi_4Ti_4O_{15}$ A = Ca, Sr, Ba and Pb. The structures were refined in the orthorhombic space group $A2_1am$. The panels to the right illustrates the 215 reflection that is forbidden in $I4/mmm$. The progressive increase in intensity of this reflection reflects the greater tilting of the TiO_6 octahedra.

patterns are illustrated in Figs. 1 and 3 whilst Table 1 presents a summary of the refinement conditions and Tables 2–5 the refined structural parameters.

3. Results and discussion

The structural refinements demonstrated the presence of the *A*-type cation (Sr, Pb, Ba) within the Bi_2O_2 layers. The amount of the alkaline earth cation within the Bi_2O_2 layers is apparently dependent on the size of the cation increasing from zero in CBT-4 to 28% in BBT-4. This increase is similar to that observed in the two layer oxides [11,13]. This increase is consistent with the observed increase in the average Bi–O bond distance for Bi(3), that is the Bi within the Bi_2O_2 layer, as the ionic radii of the *A*-type cation increased, see Table 6. The results for PBT-4 suggest even greater disorder with 40% of the Bi(3) site occupied by Pb. This not unexpected given both Pb^{2+} and Bi^{3+} have a $6s^2$ lone pair electron configuration, and extensive disorder has been observed in $PbBi_2Nb_2O_9$ [30]. The remainder of the *A*-type cation appears to be randomly distributed over the perovskite-like Bi(1) and Bi(2) sites for CBT-4, SBT-4 and BBT-4. The results for PBT-4 appear anomalous in that no Pb is found in the Bi(1) site. These occupancies are consistent with the observation that the average Bi–O bond distances for the two perovskite-like A-sites Bi(1) and Bi(2)

Table 1
Details of structure refinements

	$CaBi_4Ti_4O_{15}$	$SrBi_4Ti_4O_{15}$	$PbBi_4Ti_4O_{15}$	$BaBi_4Ti_4O_{15}$
Space group	*A*2$_1$*am*	A2$_1$*am*	A2$_1$*am*	A2$_1$*am*
Cell parameters				
a (Å)	5.4329(2)	5.4509(3)	5.4535(2)	5.4697(2)
b (Å)	5.4113(2)	5.4373(3)	5.4312(2)	5.4558(2)
c (Å)	40.721(17)	41.005(22)	41.415(13)	41.865(11)
X-ray (0.5010 Å) $2\theta = 1$–40°				
R_p (%)	3.99	3.82	4.46	3.44
R_{wp} (%)	5.80	5.65	4.50	4.90
X-ray (0.8504 Å) $2\theta = 4.4$–80°				
R_p (%)	2.77	2.50	2.24	2.19
R_{wp} (%)	4.27	3.67	2.89	2.82
Neutron (1.4925 Å) $2\theta = 6$–150°				
R_p (%)	5.64	6.02	4.50	4.35
R_{wp} (%)	6.89	7.74	5.69	5.32

Table 2
Refined structural parameters of $CaBi_4Ti_4O_{15}$

Atom	*x*	*y*	*z*	B_{iso} (Å^2)	*N*
Bi1/Ca	0.25	0.2538(9)	0	1.99(6)	0.676(4)
Bi2	0.2613(15)	0.2445(6)	0.10423(3)	1.99(4)	0.765(2)
Bi3/Ca	0.2487(7)	0.2646(5)	0.2188(2)	1.90(3)	1
Ti1	0.2621(12)	0.2439(15)	0.5485(1)	0.62(6)	1
Ti2	0.2290(14)	0.2547(15)	0.3488(1)	1.34(9)	1
O1	0.2767(21)	0.2125(13)	0.5	1.20(11)	1
O2	0.5919(15)	0.5613(7)	0.0522(1)	0.51(6)	1
O3	0.2939(15)	0.3081(7)	0.4026(1)	0.37(6)	1
O4	0.5145(16)	0.4914(9)	0.1390(1)	0.46(5)	1
O5	0.2589(20)	0.2198(9)	0.3010(1)	1.45(6)	1
O6	0.4963(18)	0.4941(8)	0.2502(1)	0.93(6)	1
O7	−0.0117(19)	−0.0205(10)	0.0438(1)	1.65(8)	1
O8	0.0485(15)	0.0298(9)	0.1453(1)	0.93(8)	1

Table 3
Refined structural parameters of $SrBi_4Ti_4O_{15}$

Atom	*x*	*y*	*z*	B_{iso} (Å^2)	*N*
Bi1/Sr	0.25	0.2600(24)	0	0.66(9)	0.81(1)
Bi2	0.256(3)	0.2394(16)	0.1051(2)	1.37(7)	0.83(1)
Bi3/Sr	0.248(3)	0.2582(13)	0.2189(1)	1.24(5)	0.98(1)
Ti1	0.270(3)	0.251(5)	0.4507(1)	0.3(1)	1
Ti2	0.247(3)	0.246(3)	0.3466(1)	0.1(1)	1
O1	0.297(4)	0.197(3)	0.5	0.5(2)	1
O2	0.558(4)	0.5351(24)	0.0488(3)	1.5(2)	1
O3	0.302(3)	0.2967(22)	0.4001(2)	0.3(2)	1
O4	0.508(3)	0.4919(29)	0.1394(2)	1.3(2)	1
O5	0.244(4)	0.2255(25)	0.2999(2)	1.7(2)	1
O6	0.510(4)	0.4966(22)	0.2504(3)	1.4(1)	1
O7	−0.006(4)	−0.0292(27)	0.0452(3)	1.6(2)	1
O8	0.014(5)	0.012(4)	0.1472(3)	2.6(3)	1

Table 4
Refined structural parameters of $PbBi_4Ti_4O_{15}$

Atom	*x*	*y*	*z*	B_{iso} (Å^2)	*N*
Bi1/Pb	0.25	0.2490(9)	0	1.96(4)	1
Bi2	0.2481(16)	0.2497(6)	0.10541(8)	1.77(3)	0.34(4)
Bi3/Pb	0.2542(12)	0.2532(6)	0.21949(7)	1.60(2)	0.59(5)
Ti1	0.2706(15)	0.2505(16)	0.4502(2)	0.60(4)	1
Ti2	0.2649(15)	0.2462(9)	0.3467(1)	0.49(4)	1
O1	0.2987(15)	0.2011(10)	0.5	1.90(9)	1
O2	0.5893(12)	0.5467(6)	0.0503(1)	1.66(6)	1
O3	0.3039(13)	0.2908(8)	0.4014(1)	1.92(7)	1
O4	0.5157(14)	0.4897(9)	0.1408(1)	1.03(5)	1
O5	0.2680(15)	0.2266(10)	0.3034(1)	2.58(6)	1
O6	0.5097(14)	0.5022(8)	0.2520(1)	1.39(4)	1
O7	0.0292(16)	−0.0037(11)	0.0434(1)	2.44(7)	1
O8	0.0466(12)	0.0136(7)	0.1457(1)	0.81(5)	1

Table 5
Refined structural parameters of $BaBi_4Ti_4O_{15}$

Atom	*x*	*y*	*z*	B_{iso} (Å^2)	*N*
Bi1/Ba	0.25	0.249(4)	0	3.5(1)	0.20(1)
Bi2	0.2740(21)	0.248(3)	0.10646(8)	3.7(6)	0.69(1)
Bi3/Ba	0.2827(13)	0.249(3)	0.2198(7)	2.5(5)	0.72(1)
Ti1	0.283(3)	0.251(3)	0.4498(1)	0.56(9)	1
Ti2	0.301(2)	0.249(2)	0.3456(1)	0.22(10)	1
O1	0.282(3)	0.177(3)	0.5	2.9(3)	1
O2	0.499(2)	0.457(1)	0.0481(2)	3.5(4)	1
O3	0.259(3)	0.260(2)	0.4045(1)	1.9(1)	1
O4	0.531(2)	0.491(2)	0.1436(2)	1.2(1)	1
O5	0.270(3)	0.243(2)	0.3044(1)	1.5(1)	1
O6	0.537(3)	0.498(1)	0.2496(2)	1.0(1)	1
O7	0.016(3)	−0.028(2)	0.0449(2)	2.5(3)	1
O8	0.028(2)	−0.008(2)	0.1430(2)	1.5(3)	1

Table 6
Comparison of ionic radii (Å) of A^{2+} ions coordinated to 12 oxygen ions with selected structural and physical properties for the $ABi_4Ti_4O_{15}$ oxides

A	Ca	Sr	Pb	Ba
Ionic radius (Å)	1.34	1.44	1.49	1.61
t	0.97	1.00	1.02	1.08
$2(a-b)/(a+b) = E_t$	0.001992	0.001249	0.002049	0.001272
T_c (K)	1090	820	840	670
P_s μC cm^{-2}	33.7	25.0	27.5	20.9
A(1)–O_{av} (Å)	2.74	2.73	2.75	2.75
BVS A(1)	2.56	2.57	2.57	2.29
A(2)–O_{av} (Å)	2.74	2.76	2.78	2.80
BVS A(2)	2.95	2.64	2.65	2.30
A(3)–O_{av} (Å)	2.97	2.96	3.00	3.03
BVS A(3)	2.99	2.92	2.85	2.75
Ti(1)–O_{av} (Å)	1.98	1.99	1.99	1.98
BVS Ti(1)	3.89	3.82	3.79	3.97
Ti(1)–O_{av} (Å)	2.02	2.01	2.00	2.03
BVS Ti(2)	3.82	3.69	3.95	3.93
Ti(1)–O(3)–Ti(2)	157.1(8)	161.6(1.2)	163.7(6)	170.7(9)

The tolerance factor, t, and bond valence sums (BVSs) were calculated assuming there is no cation disorder with the ionic radii of six-coordinate Ti^{4+} being 0.605 Å and for O^{2-} it is 1.40 Å.

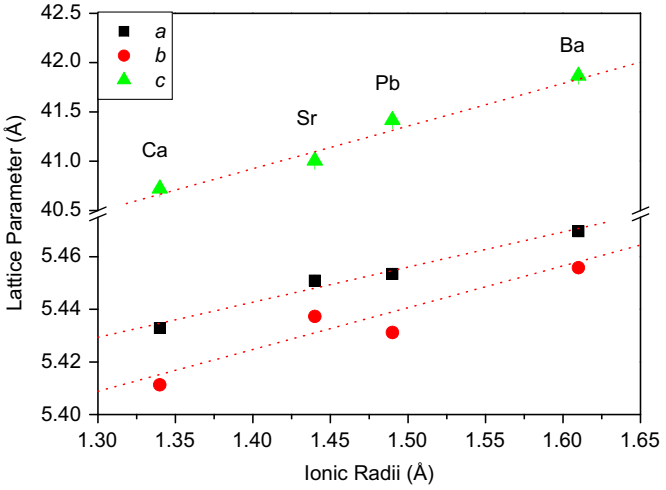

Fig. 4. Lattice constants of $ABi_4Ti_4O_{15}$ (A = Ca, Sr, Pb and Ba) plotted against the ionic radii of the A^{2+} ions. The broken lines serve as a guide to the eye to illustrate the anomalous behavior of the A = Pb sample.

were only weakly dependent on the identity of the A-type cation.

The bond valence sums (BVSs) for the three Bi sites provide further evidence for the existence of cation disorder. The BVS for the Bi(1) site in CBT-4, calculated assuming the site is fully occupied by Bi^{3+}, is 2.56 suggesting a appreciable amounts of the divalent Ca cation are on this site. Conversely the BVS for the Bi(2) and Bi(3) sites demonstrate these are predominantly occupied by a trivalent cation. The BVS for the Bi(3) site remains close to three in all four compounds indicating that this site contains little divalent cation whereas the BVS for the Bi(1) and Bi(2) sites are indicative of mixed occupancy, with the BVS for the Bi(1) site in BBT-4 being the lowest. The BVS for the two Ti cations are as expected for tetravalent Ti cations.

As shown in Fig. 4 the lattice parameters increased as the size of the A-type cation increased. The lead compound is clearly anomalous in this series and this possibly reflects either the difference in the nature of the cation disorder as described above or is a consequence of differences in bonding interactions of Pb^{2+} compared to the alkaline earth cations. The extent of the orthorhombic distortion can be quantified as $2(a-b)/(a+b)$ and this does not show a systematic variation with the size of the A-type cation, Table 6. Visual examination of the diagnostic reflections, Fig. 1, suggested that there was no systematic dependence of the distortion from the archetypal tetragonal structure on the size of the A-type cation. It is possible that the lack of a simple trend reflects the cation disorder and size of the A-type cations acting in an opposite sense. The orthorhombic distortion in the Ca (1.34 Å) and Pb (1.49 Å) compounds is clearly larger than for the Sr (1.44 Å) and Ba (1.61 Å) compounds. Here the figures in parenthesis are the ionic radii of the A-type cation in a 12-coordinate environment [31].

The mismatch in size between the A-type and Ti cations in the $ABi_4Ti_4O_{15}$ structure results in tilting of the TiO_6 octahedra and it is this tilting that results in a lowering of symmetry from tetragonal to orthorhombic. The tilting of MO_6 octahedra in perovskites has been described in considerable detail by Glazer and others [32,33]. Suffice to say there are two situations, where successive MO_6 octahedra in a particular crystallographic orientation rotate in the same sense (in-phase) or in the opposite sense (out-of-phase). A low symmetry perovskite can have three independent tilts. A further complication evident, from Fig. 2, is that there are two types of TiO_6 in the $ABi_4Ti_4O_{15}$ structure that are referred to as the "inner" $Ti(1)O_6$ and "outer" $Ti(2)O_6$ octahedra. The outer octahedra are considerably more distorted than the inner octahedra and are characterized by an extremely short Ti–O axial bond directed towards the Bi_2O_2 layers and a long Ti–O bond towards the inner $Ti(1)O_6$ octahedra. These distances reflect the displacement of the Ti atom towards the Bi_2O_2 layers. Whilst the rotations of the $Ti(1)O_6$ and $Ti(2)O_6$ octahedra are in-phase, the rotations of these the octahedra are out-of-phase with each other.

The structural challenge in the four-layer oxides is to optimize the bonding between the Bi_2O_2 and $[ABi_2Ti_4O_{13}]$ layers. Variable temperature studies of numerous ABO_3 perovskites, including $NaTaO_3$ [34,35] and $CaTiO_3$ [36] have demonstrated that tilting about the c-axis invariably reduces the a- and b-axis, and there is a consequent expansion in the c-axis. That tilting promotes anisotropic expansion of the cell is also apparent for the present structures. The volume expansion on replacing Ca in CBT-4 with Ba in BBT-4 is around 4% and this occurs predominantly along the c-axis, 2.8% expansion, with the expansion in the a- and b-direction being noticeably less, ca

0.7% and 0.8%, respectively. Despite the increase in the *ab*-plane the average Bi(3)–Bi(3) separation within the Bi_2O_2 layers actually decreases from ~3.70 Å in CBT-4 to ~3.67 Å in BBT-4. This minimal change reflects the lack of flexibility in this layer. The Bi(3) atoms in the Bi_2O_2 layers connect with the $[ABiTi_4O_{13}]$ layers via the O(5) atoms, and as a result of the TiO_6 tilting there are alternating long–short–long O(5)–O(5) contacts. The average O(5)–O(5) separation remains relatively constant changing from 3.50(1) and 4.20(2) Å {average 3.85 Å} in CBT-4 to 3.75(2) and 3.98(2) Å {average 3.87 Å} in BBT-4. In the absence of tilting there would only be a single O(5)–O(5) separation. Clearly tilting acts to optimize the match between the two layers.

The requirement to maintain a near constant "bite" due to the interaction between the $Ti(2)O_6$ groups and the Bi_2O_2 layer limits the flexibility of the Ti(2)–O(8)–Ti(2) moiety. Changes in the precise geometry of the inner $Ti(1)O_6$ octahedra are expected to have little influence on the separation of the O(5) anions at the interface between the two layers. Consequently the Ti(1)–O(3)–Ti(2) angle shows the largest sensitivity to the *A*-type cation, since this acts as a flexible connection between the rigid $Ti(1)O_6$ and the Bi_2O_2 layers.

4. Variable temperature studies

The temperature dependences of the structures of the four compounds were investigated using synchrotron X-ray powder diffraction data collected at 0.5 Å. These results are summarized in Fig. 5 which shows a gradual reduction in the orthorhombic splitting for all four compounds as the temperature is increased. The symmetry of the structures was established from both the observation of splitting and the appearance of diagnostic superlattice reflections. In the case of CBT-4 heating to above 950 K results in loss of the orthorhombic distortion. Whilst the intensity of the 015 reflection decreases as the temperature is increased it remains apparent to the highest temperature measured, 1000 K, demonstrating the structure remains orthorhombic until this temperature. This is consistent with the reports that the Curie temperature for CBT-4 is 1090 K [16]. For both SBT-4 and PBT-4 the intensity of the 015 reflection is observed to become vanishingly small as the temperature increases, and in both cases the intensity associated with this reflection is no longer observable at the same point the structure becomes metrically tetragonal. Evidently both SBT-4 and PBT-4 undergo a transition to tetragonal upon heating. The diffraction patterns of SBT-4

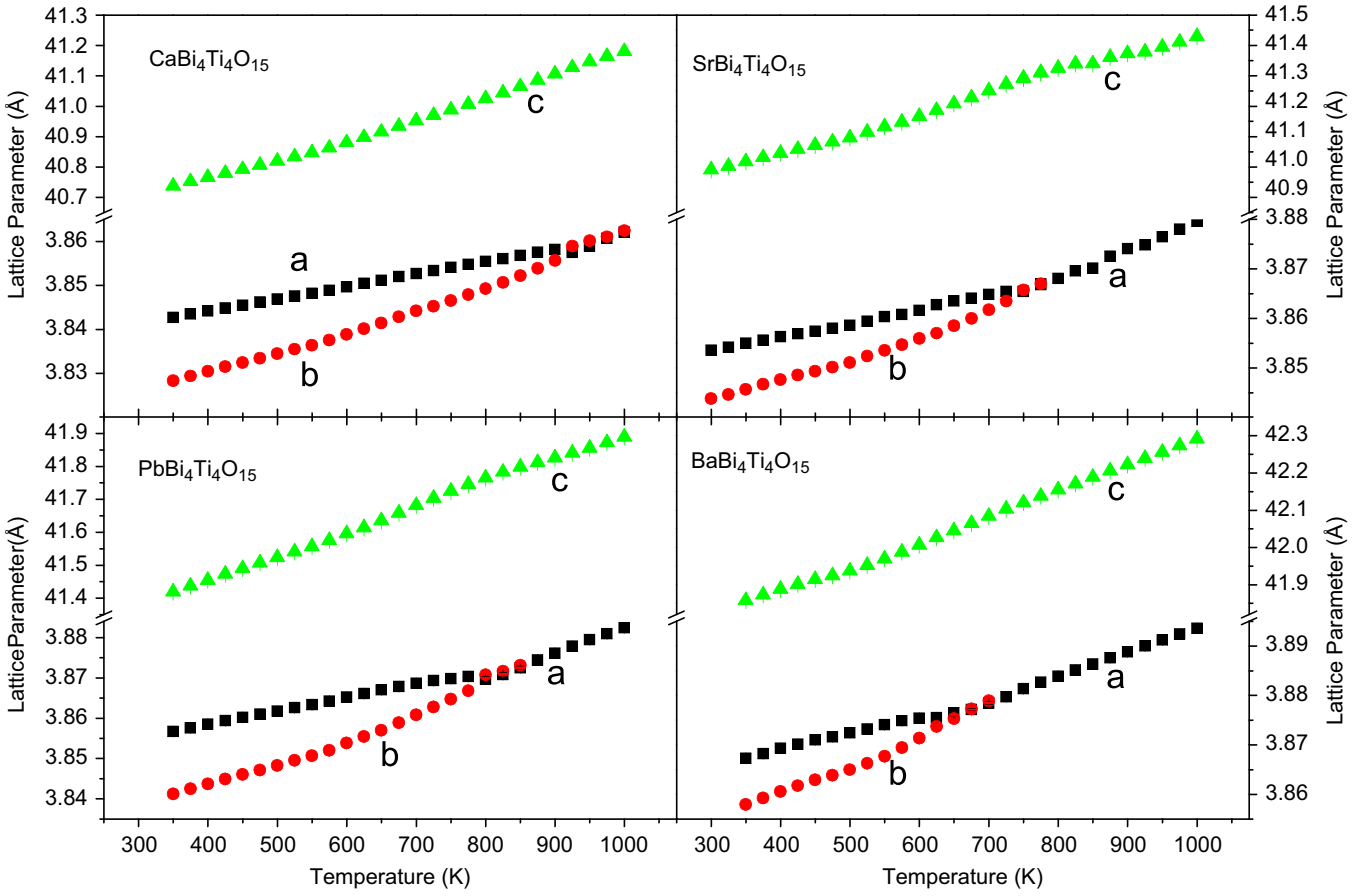

Fig. 5. Temperature dependence of the lattice parameters for the four oxides $ABi_4Ti_4O_{15}$ A = Ca, Sr, Ba and Pb estimated from synchrotron X-ray diffraction data. The *a*- and *b*-lattice parameters in the low temperature orthorhombic structure have been scaled to those seen in the high temperature tetragonal structure.

and PBT-4 recorded at temperature above 825 and 875 K, respectively, were well fitted using the space group $I4/mmm$. These temperatures are in remarkably good agreement with the reported Curie temperatures of 820 and 840 K, respectively [16]. The observation of a structural transition in PBT-4 is in conflict with the results of Nalini and Guru Row [17] who suggested that this material does not undergo a phase transition below 873 K.

The temperature dependence of the structure of BBT-4 has been described previously [21] and we simply note that for this oxide the diagnostic 015 reflection is not observed, and the transition to the tetragonal structure is based solely on the variation in the cell metric. The transition to tetragonal occurs near 725 K, which is slightly higher than the reported Curie temperature of 670 K [18]. It was not possible to establish if a paraelectric phase exists between 670 and 725 K, or if this reflects differences in the thermometry of the two measurements.

The temperature dependence for the orthorhombic strains for the four oxides were calculated as $(a-b)/(a+b)$, and these are illustrated in Fig. 6. There are a number of features worthy of comment from in this figure. Firstly we observe the strain to vary linearly with temperature for the three alkaline earth containing samples (CBT-4; SBT-4 and BBT-4), although for BBT-4 there is an obvious discontinuity in the strain near 550 K, that is possibly associated with a transition to a paraelectric orthorhombic structure. For both CBT-4 and SBT-4 the strains provide no evidence for such a transition. Failure to observe this, suggests the major contribution to the strain is the out-of-phase tilting of the corner sharing TiO_6 octahedra, rather than the cation displacements that drive the ferroelectric behavior. Whereas CBT-4 and SBT-4 both exhibit a sharp transition typical of a "normal" ferroelectric, BBT-4 displays a broad transition indicative of relaxor-like ferroelectric behavior [18]. The stain anomaly in BBT-4 is thought to reflect the relaxor-like behavior. Tellier et al. [20] have suggested that this difference in behavior is a consequence of the differences in cation disorder. We have some reservations regarding this conclusion extensive cation disorder is observed in the $n = 2$ oxides that are normal ferroelectrics and we find evidence for cation disorder, albeit at a very low level, in SBT-4. Gelfulso et al. have demonstrated that the ferroelectric response of bulk SBT-4 is sensitive to sample preparation methods [37], with a similar sensitivity observed for thin-films [38]. It is feasible that the extent of cation disorder may be sensitive to the thermal history of the sample.

The behavior of PBT-4 illustrated in Fig. 6 is clearly different to that observed for the other three samples, and there is a clear discontinuity in the strain near 600 K whereas the structure does not become tetragonal until near 800 K. The Curie temperature for PBT-4 is reported to be around 875 K which is in reasonable agreement with the

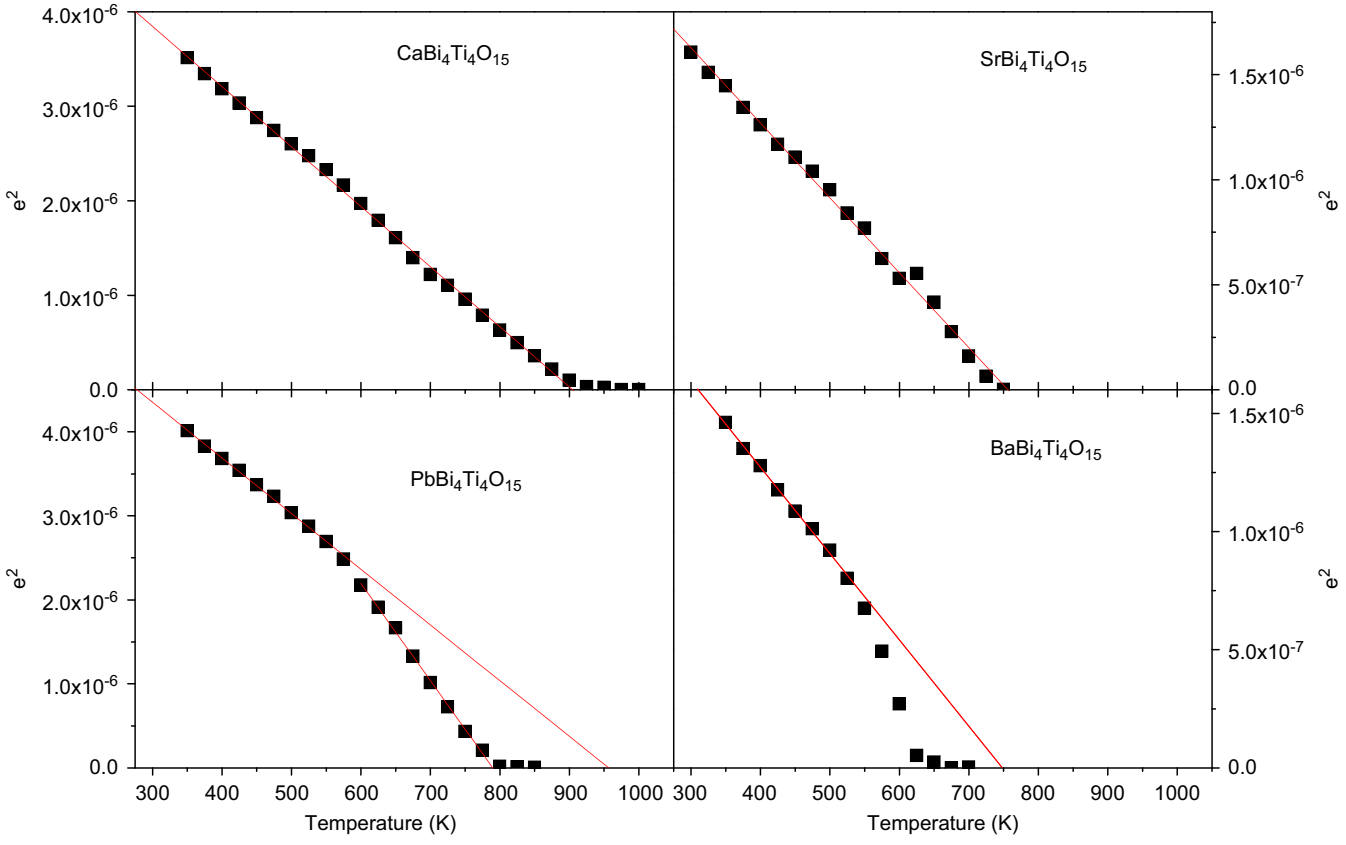

Fig. 6. Temperature dependence of the square of the orthrhombic strains for the four oxides $ABi_4Ti_4O_{15}$ A = Ca, Sr, Ba and Pb estimated from synchrotron X-ray diffraction data.

temperature observed for the structural transition, suggesting the feature near 600 K is not associated with the ferroelectric properties of this oxide. If the suggestion that the strains are predominately derived from the octahedral tilting is correct then this suggests that the presence of Pb^{2+} in the structure has a unique (compared to the alkaline earth cations) impact on the tilting. It is possible that the $6s^2$ lone pair electrons of the Pb cation are somehow involved and it is tempting to postulate that there is disorder of the Pb^{2+} cations, similar to that seen in $PbZrO_3$ [39]. An alternate possibility is that the material has undergone a continuous transition to a second orthorhombic ferroelectric structure. Group theory suggests this would be in *Fmm*2. Variable temperature neutron diffraction studies are required to better understand the origin of this feature in the strains.

5. Conclusions

In summary we now consider the four general observations regarding the $n = 2$ oxides $ABi_2M_2O_9$ M = Nb or Ta made in the introduction. As in the $n = 2$ oxides we observe cation disorder between the perovskite A-type and layer Bi cations. The extent of this disorder depends on the size and electronic configuration of the A-type cation. Secondly reducing the size of the A-type cation introduces tilting of the TiO_6 octahedra, however, unlike the $n = 2$ oxides such tilting is evident in the Ba containing oxides. Thirdly, calculation of the spontaneous polarizations using the point charge model demonstrates that this is due to displacement of the perovskite cations along the a-axis, as also occurs in the $n = 2$ oxides.

Finally, the diffraction data demonstrates that the ferroelectric phase has the orthorhombic space group $A2_1am$ and that heating this results in a transition to a tetragonal paraelectric structure for A = Sr, Pb and Ba. The transition to the paraelectric phase in CBT-4 occurs at temperatures above that achieved in the present measurements. However, we find no conclusive evidence for the existence of an orthorhombic paraelectric phase as observed in the $n = 2$ oxides. The group theoretical analysis of Macquart et al. [9] shows a continuous transition to $I4/mmm$ must involve an intermediate phase, and in the $n = 2$ oxides this is observed to exist in space group *Amam*. If such a phase exists in the four layer oxides, it does so over a much narrower temperature range than seen in the $n = 2$ oxides.

Acknowledgments

This work was partially supported by the Australian Research Council and the Access to Major Research Facilities program. The measurements at SPring-8 were carried out under proposal 2002B0001. The work performed at the Australian National Beamline Facility was supported by the Australian Synchrotron Research Program, which is funded by the Commonwealth of Australia under the Major National Research Facilities program. The Australian Institute of Nuclear Science and Engineering supported the neutron diffraction experiments. The assistance of Dr Brett Hunter with the collection of the neutron diffraction data is gratefully acknowledged.

References

[1] C. A-Paz de Araujo, J.D. Cuchiaro, L.D. Mcmillan, M.C. Scott, J.F. Scott, Nature 374 (1995) 627.
[2] B.H. Park, B.S. Kang, S.D. Bu, T.W. Noh, J. Lee, W. Jo, Nature 401 (1999) 682.
[3] R.K. Graselli, Top. Catal. 21 (2002) 79.
[4] R. Funahashi, I. Matsubara, S. Sodeoka, Appl. Phys. Lett. 76 (2000) 2385.
[5] L.T. Sim, C.K. Lee, A.R. West, J. Mater. Chem. 12 (2002) 17.
[6] B. Aurivillius, Ark. Kemi. 1 (1949) 463–499.
[7] Y. Arimoto, H. Ishiwara, MRS Bull. 29 (2004) 823.
[8] R.L. Withers, J.G. Thompson, A.D. Rae, J. Solid State Chem. 94 (1991) 404.
[9] R. Macquart, B.J. Kennedy, B.A. Hunter, C.J. Howard, Y. Shimakawa, Integrated Ferroelectrics 44 (2002) 101.
[10] R. Macquart, B.J. Kennedy, B.A. Hunter, C.J. Howard, J. Phys. Condens. Matter 14 (2002) 7955.
[11] S.M. Blake, M.J. Falconer, M. McCreedy, P. Lightfoot, J. Mater. Chem. 7 (1997) 1609.
[12] Y. Shimakawa, Y. Kubo, Y. Nakagawa, S. Goto, T. Kamiyama, H. Asano, F. Izumi, Phys. Rev. B 61 (2000) 6559.
[13] R.B. Macquart, B.J. Kennedy, Y. Shimakawa, J. Solid State Chem. 160 (2001) 174.
[14] C.H. Hervoches, J.T.S. Irvine, P. Lightfoot, Phys. Rev. B 64 (2001) 100102(R).
[15] M.E. Fuentes, A. Mehta, L. Lascano, H. Camacho, R. Chianelli, J.F. Fernandez, L. Fuentes, Ferroelectrics 269 (2002) 159.
[16] G.A. Smolenski, V.A. Bokov, V.A. Isupov, N.N. Krainik, R.E. Pasynkov, A.I. Sokolov, in: G.A. Smolenski (Ed.), Ferroelectrics and Related Materials, vol. 3, Gordon and Breach Science Publishers, London, 1984.
[17] G. Nalini, T.N.G. Row, Bull. Mater. Sci. 25 (2002) 275.
[18] H. Irie, M. Miyayama, T. Kudo, J. Appl. Phys. 90 (2001) 4089.
[19] S. Kojima, R. Imaizumi, S. Hamazaki, M. Takashige, J. Mol. Struct. 348 (1995) 37.
[20] J. Tellier, P. Boullay, M. Manier, D. Mercurio, J. Solid State Chem. 177 (2004) 1829.
[21] B.J. Kennedy, Y. Kubota, B.A. Hunter, Ismunandar, K. Kato, Solid State Commun. 126 (2003) 653.
[22] C.H. Hervoches, A. Snedden, R. Riggs, S.H. Kilcoyne, P. Manuel, P. Lightfoot, J. Solid State Chem. 164 (2002) 280.
[23] I.M. Reaney, D. Damjanovic, J. Appl. Phys. 80 (1996) 4223.
[24] Ismunandar, T. Kamiyama, A. Hoshikawa, Q. Zhou, B.J. Kennedy, Y. Kubota, K. Kato, J. Solid State Chem. 177 (2004) 4188.
[25] T.M. Sabine, B.J. Kennedy, R.F. Garrett, G.J. Foran, D.J. Cookson, J. Appl. Crystallogr. 28 (1995) 513.
[26] E. Nishibori, M. Takata, K. Kato, M. Sakata, Y. Kubota, S. Aoyagi, Y. Kuroiwa, M. Yamakata, N. Ikeda, Nucl. Instrum. Methods Phys. Res. A 467–468 (2001) 1045.
[27] C.J. Howard, C.J. Ball, R.L. Davis, M.M. Elcombe, Aust. J. Phys. 36 (1983) 507.
[28] C.J. Howard, B.A. Hunter, A Computer Program for Rietveld Analysis of X-ray and Neutron Powder Diffraction Patterns, Lucas Heights Research Laboratories, NSW, Australia, 1998, pp. 1–27.
[29] R. Macquart, B.J. Kennedy, T. Vogt, C.J. Howard, Phys. Rev. B 66 (2002) 212102.
[30] Ismunandar, B.A. Hunter, B.J. Kennedy, Solid State Ionics 112 (1998) 281.
[31] R.D. Shannon, Acta Crystallogr. A 32 (1976) 751.

[32] A.M. Glazer, Acta Crystallogr. B 28 (1972) 3384;
A.M. Glazer, Acta Crystallogr. B 31 (1975) 756.
[33] K.S. Aleksandrov, J. Bartolome, J. Phys. Condens. Matter 6 (1994) 8219.
[34] C.N.W. Darlington, K.S. Knight, Acta Crystallogr. B 55 (1999) 24.
[35] B.J. Kennedy, A.K. Prodjosantoso, C.J. Howard, J. Phys. C Condens. Matter 11 (1999) 6319.
[36] B.J. Kennedy, C.J. Howard, B.C. Chakoumakos, J. Phys. C Condens. Matter 11 (1999) 1479.
[37] M. Gelfuso, D. Thomazini, J.A. Eiras, J. Am. Ceram. Soc. 82 (1999) 2368.
[38] W.X. Xianyu, T.-Y. Won, W.I. Lee, Integrated Ferroelectrics 65 (2004) 57.
[39] D.L. Corker, A.M. Glazer, J. Dec, K. Roleder, R.W. Whatmore, Acta Crystallogr. B 53 (1997) 135.